

for this character. Turbidity is not a problem in the river, although a slight discoloration was detected in the lower slack waters. The river runs clear for most of the year except during spring runoff, flash floods and from effluents.

TABLE 2. Water chemistry for four sections of the St. Maries River.<sup>1</sup>

	West Fork	Middle Fork	Middle St. Maries	Lower St. Maries
Alkalinity (ppm)	30	30	20	25
Total Hardness (ppm)	10	20	20	20
Dissolved O <sub>2</sub> (ppm)	9	8	9	8
pH	8.9	8.9	8.9	8.8
Turbidity (J.T.U.) <sup>2</sup>	0	0	0	15

<sup>1</sup> Water chemistry analysis made 8/18/67.

<sup>2</sup> Measured in Jackson Turbidity Units.

### Summary

Algae were collected from 28 stations on the St. Maries River. Four Divisions and 34 genera were represented (number does not include diatom complex). Chlorophyta was the most widely represented. Many algae showed wide distribution in the drainage. However, *Chlamydomonas*, *Chlorella*, and *Closteriopsis* were collected only from the headwaters of the West Fork.

Characteristics of the habitat as riffles, pools, current speed, bottom type, submerged logs and vegetation influenced distribution.

No positive correlation could be made between algae distribution and pH, alkalinity, total hardness, dissolved oxygen or turbidity. An increase in abundance of algae was noted through the middle and lower portions of the river and was probably due to organic enrichment.

### Literature Cited

- Blum, J. L. 1960. Algae Populations in Flowing Waters. (In Ecology of Algae. Special Pub. No. 2.) Pymatuning Laboratory of Field Biology, Univ. of Pittsburgh. pp. 11-20.
- Flowers, S. Undated. The Algae of Utah. Unpublished Manual. Dept. of Botany, Univ. of Utah. 70 p.
- Prescott, G. W. 1962. Algae of the Western Great Lakes Area. Wm. C. Brown, Co., Dubuque, Iowa. 977 p.
- Smith, G. M. 1950. The Fresh-Water Algae of the United States. McGraw-Hill Book Company, Inc., New York. 719 p.
- Travis, W. I., H. A. Waite and J. F. Santos. 1964. Water Resources. (In Mineral and Water Resources of Idaho.) U.S. Government Printing Office, Washington, D.C. pp. 255-335.
- Whitford, L. A. 1960. Ecological Distribution of Fresh-Water Algae. (In Ecology of Algae, Special Pub. No. 2.) Pymatuning Laboratory of Field Biology, Univ. of Pittsburgh. pp. 2-7.

Accepted for publication January 28, 1969.

Walter E. Edelman, Jr.

Department of Mechanical Engineering  
California State College at Long Beach  
Long Beach, California

and

Hans J. Dahlke

Department of Mechanical Engineering  
Oregon State University  
Corvallis, Oregon

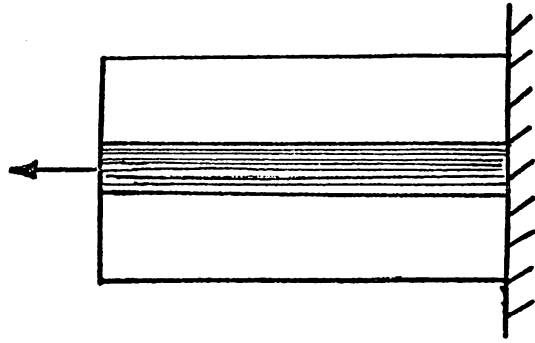
## Photoelastic Study of Stresses in a Composite Material

Interest in stress transfer mechanisms in composite materials has been high during the past few years. This interest has been expressed as a study of the stress field surrounding the stiffener in the composite material while the material is subjected to tensile loads. Various investigators have taken different approaches to the problem depending on their background. Although the techniques used by the metallurgist, the theoretical elastician, the experimental elastician, and other investigators differ, each makes its own unique contribution and each has certain limitations. The work of one investigator usually supplements or clarifies the work of a previous investigator.

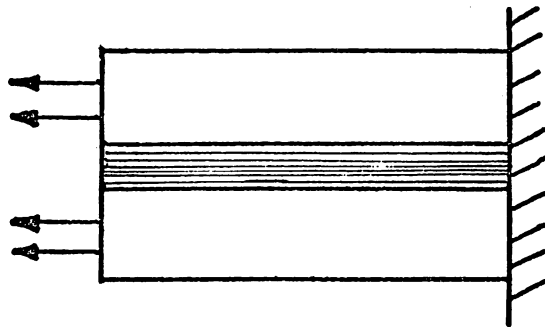
Usually the difficulties and uncertainties encountered in the study of whisker-stiffened composite materials occur in the mathematical or physical model selected for analysis. The mathematical model requires that certain simplifying assumptions be made in order to arrive at a solution. These assumptions often prevent the evaluation of the stress field at the region of the extreme stress—the region of interest to the engineer. Experimental analysis using prototype materials is handicapped by the small size of the whisker and the opacity of the matrix. In a scaled up macroscopic model there has always been a question of what factors can be successfully handled in the scaling process. For example, investigators working with the prototype materials are quite concerned with the interfacial energies associated with the boundary between the stiffener and the matrix. It is questionable whether such a factor can be successfully scaled up and used in a photoelastic experiment.

An engineer using composite materials would be interested in certain design aspects of the material. The magnitude of the stresses is of prime concern to the engineer, especially if the material is to undergo cyclic loading. High stress concentrations could lead to fatigue failure. The designer is also concerned with the ineffective or transfer length of the stiffener and the range of influence that the stiffener has on the stress field extending into the matrix. The last two quantities aid the designer in selecting the volume fraction of stiffener necessary to achieve adequate strength in the composite material.

A starting point for the above quantities is the behavior of a single stiffener, uniaxially loaded, and surrounded by a quantity of matrix so sufficient that the edge effects may be neglected. The model selected may be visualized as a cylindrical stiffener embedded concentrically in a cylindrical matrix. Loads are applied to the



Load applied to stiffener



Load applied to matrix

Figure 1. The models used in Dow's analysis.

ends of the matrix cylinder with the direction of loading along the longitudinal axis of the cylinder.

Several people have analyzed such a model. Dow has provided an analytical approach based on elastic theory (Dow, 1963). His model assumed a cylindrical stiffener surrounded by a concentric cylinder of the matrix material. Due to singularities at the end of the stiffener, he assumed that the end of the stiffener carried no load, and the load was applied entirely to either the stiffener or the matrix, but not to both (Figure 1). While this model allowed an analysis for the transfer of stresses along the stiffener-matrix interface, it did not provide a means for evaluating the maximum stresses occurring near the tip of the stiffener. The difficulties involved

in the analysis of stresses near the tip of the stiffener have led to several experimental studies using photoelasticity.

Tyson, in his experiment, milled a slot in a sheet of photoelastic material, fitted an aluminum stiffener to the slot and glued it in place (Tyson, 1965). The loads were applied through the matrix in such a way as to represent a semi-infinite stiffener quite similar to the model proposed by Dow, but limited to two dimensions for ease of photoelastic analysis.

Schuster used a prototype whisker embedded in a three-dimensional epoxy matrix (Schuster and Scala, 1964). The small size of the prototype whisker prohibited conventional three-dimensional slicing techniques and required a novel approach in the data reduction. The photoelastic epoxy had an elastic modulus much lower than that of matrix materials normally associated with whisker composites, giving a ratio of elastic modulus of the stiffener to that of the matrix of 150:1.

MacLaughlin made a very comprehensive study of the effect of stiffener end geometry on the shear stress at the stiffener-matrix interface (MacLaughlin, 1966). His models were geometrically scaled-up two-dimensional macromodels using steel stiffeners and an epoxy matrix. The ratio of elastic modulus of the stiffener to the matrix was 3000:1, much larger than that expected in a prototype material. In his analysis he questioned the effect of using a two-dimensional model rather than a three-dimensional model.

The purpose of this study is to examine a three-dimensional macroscopic model in which the ratio of elastic modulus of the stiffener to the matrix is controlled and in which the end of the stiffener can support a load. Information concerning the range of influence of the stiffener, as well as the maximum stresses and stress distribution along the stiffener-matrix interface, is provided. This information is expected to lay the groundwork for future projects in which the effects of parallel and transverse stiffeners can be determined.

#### Design of the Models

This investigation was designed to control the following details:

- (1) The model of the composite material was to be three-dimensional and of such size that conventional slice-analysis techniques of three-dimensional photoelasticity could be used in data reduction.
- (2) The geometry of the stiffener would be controlled to match that of prototype stiffeners.
- (3) The quantity of matrix surrounding the stiffener would be large enough to make edge effects negligible.
- (4) The ratio of the elastic modulus of the stiffener to that of the matrix would be similar to the ratio expected in the prototype material.

Requirements 2 and 4 above reduced the generality of the experiment to simulating one particular composite material. The material selected was  $\alpha$   $\text{Al}_2\text{O}_3$  (sapphire) whiskers in an aluminum matrix. This material was selected because in all likelihood it will be one of the first whisker composites to reach the engineering market and also because of the data Dow has developed for this combination (Dow, 1963; Business Week, 1966).

Item 1 was satisfied by geometrically scaling up the whisker stiffener by a factor of about 1000. The simulated stiffener had a nominal diameter of 0.080 inch.

Item 2 was determined by the method of growing and harvesting the  $\alpha\text{Al}_2\text{O}_3$  whiskers and from crystallographic data. The whiskers are grown by vapor condensation and the finished product appears as a cluster of acicular needles rising out of the boat that serves as the base during the growth phase (Krock and Kelsey, 1965). The whiskers are harvested by breaking the fixed end near the boat. The free end of the whisker appears as a needle shape and the harvested end is a broken end. From crystallographic data, it has been determined that  $\alpha\text{Al}_2\text{O}_3$  can part across either the basal [0001] or the rhombohedral [10 1] plane (Dana, 1941). This gives two possible end shapes, one perpendicular to the longitudinal axis and one that cuts the longitudinal axis at an  $18^\circ$  inclination. The angle of the free or needle shaped end is not so well known. A sample of selected  $\alpha\text{Al}_2\text{O}_3$  whiskers was examined, and it was determined that the included angle of the needle shaped end varied from  $5^\circ$  to  $6^\circ$ . These three end shapes, the square, the  $18^\circ$ , and the needle, comprised the models studied. Although the cross section of the  $\alpha\text{Al}_2\text{O}_3$  whisker is hexagonal, it was felt that no observable error would occur if a circular cross section were used in the scaled-up whisker.

Item 3 was determined by trial and error in the development of models. It was determined that the maximum range of influence was about six stiffener diameters. This gives a matrix cylinder of about one-inch diameter with the simulated stiffener of 0.080 inch diameter embedded at the center. For ease of manufacturing the cylinder of matrix had a square cross section. In order to preserve the intimate contact at the stiffener-matrix interface, the epoxy matrix was cast around the simulated stiffener. A refrigerated curing technique was used to eliminate residual isochromatics (Edelman). Due to symmetry, the models tested were cut along a plane perpendicular to the stiffener axis. This made the physical models very similar to Dow's mathematical model, with the exception that the end of the stiffener could support a load (Figure 2).

Item 4 was controlled by the selection of materials. Ciba type 502 epoxy with 20 pph of type 956 hardener was used for the matrix. The selection of this epoxy system, with its elastic modulus of 400,000 psi as the matrix, limited the materials suitable for the stiffener to those with an elastic modulus of about  $2.4 \times 10^6$  psi. Very few engineering materials have an elastic modulus in this range, and, of those available, wood was the most suitable. Selected yellow birch dowel was used for the simulated stiffener. This combination gives a ratio of elastic modulus of the stiffener to the matrix of 5:1 as compared to the 6:1 expected in the prototype material. The problem of selecting materials with Poisson's ratios similar to those expected in the prototype was considered. However, Poisson's ratio has not been determined for the prototype stiffener, and a unique value may not exist due to the orthotropic structure of the stiffener. Consequently, only the elastic modulus was considered in the selection of materials for this investigation.

#### Procedure

The following simulation technique was used in the loading phase of the experiment. The models were loaded at room temperature in tension and compression along the longitudinal axis. The formation of isochromatics was observed to be repetitive and linear with load up to 5400 psi, the limit of optical resolution. The isochromatic fringe patterns generated upon loading at room temperature were then duplicated by a creeping-in process. In this creeping-in process the models were heated to  $60^\circ\text{C}$

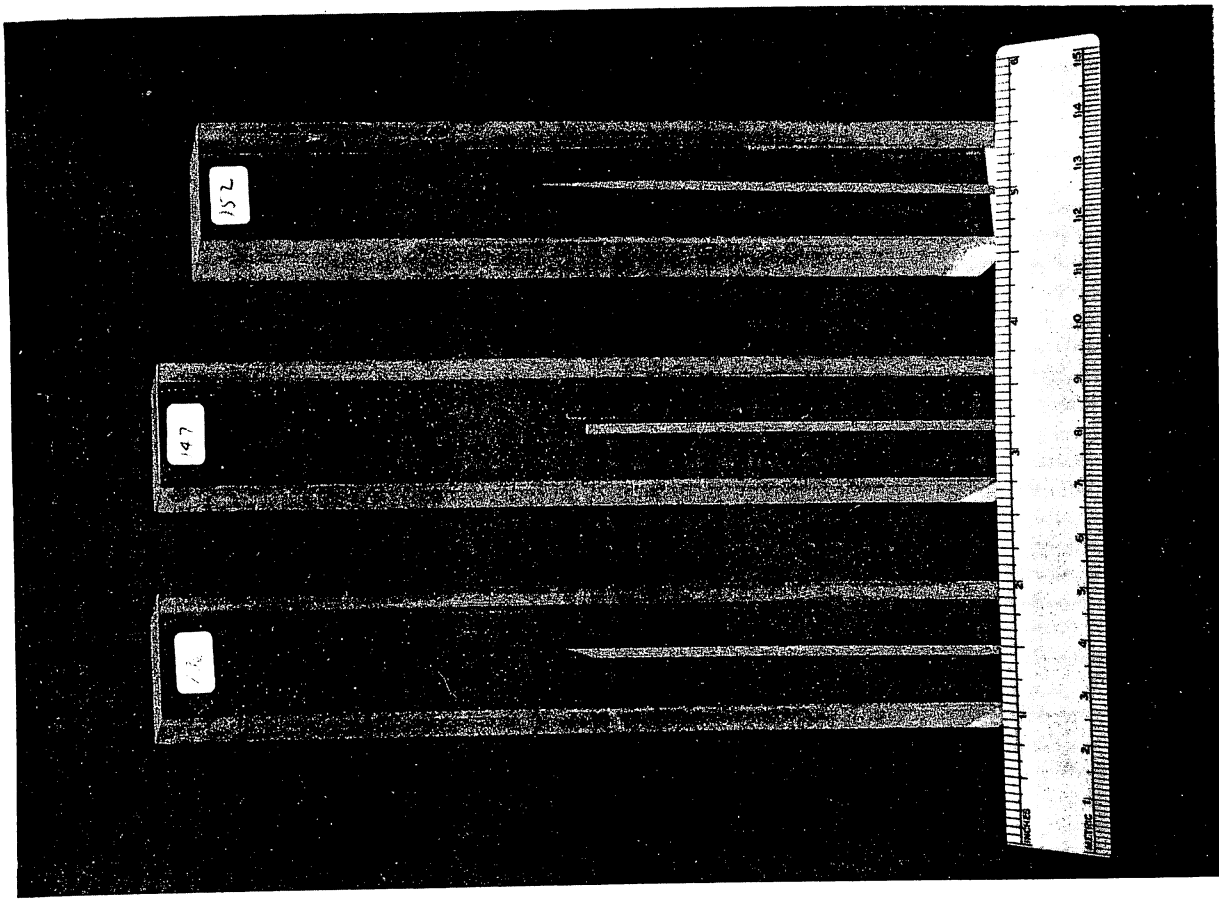


Figure 2. Typical models used in this investigation.

and strained until the isochromatics formed were observed to be generally similar to those generated by loading at room temperature. There were some differences in the angles at which the isochromatics approached the surface of the model. These differences were corrected by directing blasts of cold air onto the surface of the model while cooling them to room temperature. The cold air blasts allowed the orientation of the isochromatics near the surface of the model to be controlled.

The simulation technique described above was developed in order to avoid the effects of the decreased elastic modulus at the elevated temperature necessary for locking-in the isochromatics. The geometry of the isochromatic pattern was controlled by varying the applied strain and the cooling rate. The basic objective was to return the model to room temperature with a locked-in isochromatic pattern which duplicated the isochromatic pattern generated by loading at room temperature.

Since the 60°C temperature used was below the critical or stress-freezing temperature of the epoxy, the isochromatics were subjected to creep. The locked-in pattern remained stable for about 10 days. Because the analysis of a model was completed in less than one day, creep was not a problem in this experiment.

After the model had been returned to room temperature with the isochromatics locked-in, a slice approximately 0.10 inch thick was taken from the model. The slice was in the plane of the stiffener and contained the stiffener. The slice was cut out on a hand saw and the rough surfaces were smoothed on a milling machine using a single pass of a wide-faced cutter. The milled surface was sufficiently smooth that a coating of silicone oil improved the optical clarity enough for analysis on a Photoelastic Type 052 polariscope (Figure 3).

The slice thickness of 0.10 inch was selected on the basis of previous experiments. The ideal approach is to use a slice of infinitesimal thickness in order to obtain a true two-dimensional field. The experimental approach requires that the slice be thick enough to yield a sufficiently high fringe order for analysis and be strong enough to withstand normal handling. The problem of selecting an appropriate slice thickness was approached by taking a three-dimensional model and milling successive layers off two opposing sides, giving a slice of decreasing thickness. It was found that when the thickness of the slice fell below 1.5 stiffener diameters the fringe geometry was constant and the fringe order was directly proportional to the thickness. By selecting a slice thickness slightly greater than the diameter of the stiffener, the problem of milling along the interface of two materials was avoided.

#### Data Presentation

The shear stress in the matrix at the stiffener-matrix interface was determined photoelastically. This stress was normalized by dividing it by the applied normal stress. These data are then presented as stress concentration factors. It was observed during the loading phase that certain regions had high stresses and steep shear stress gradients, and were subject to the initiation of stress cracks. The stress concentration along the direction of the steepest gradient is given in terms of shear stress divided by applied normal stress. The direction in question starts at the tip of the stiffener and radiates outward along a line perpendicular to the stiffener. A similar set of data for stress concentration across the region of the maximum influence of the stiffener is also given. Again, the direction is perpendicular to the stiffener, but the location with respect to the tip of the stiffener varies from one to three stiffener

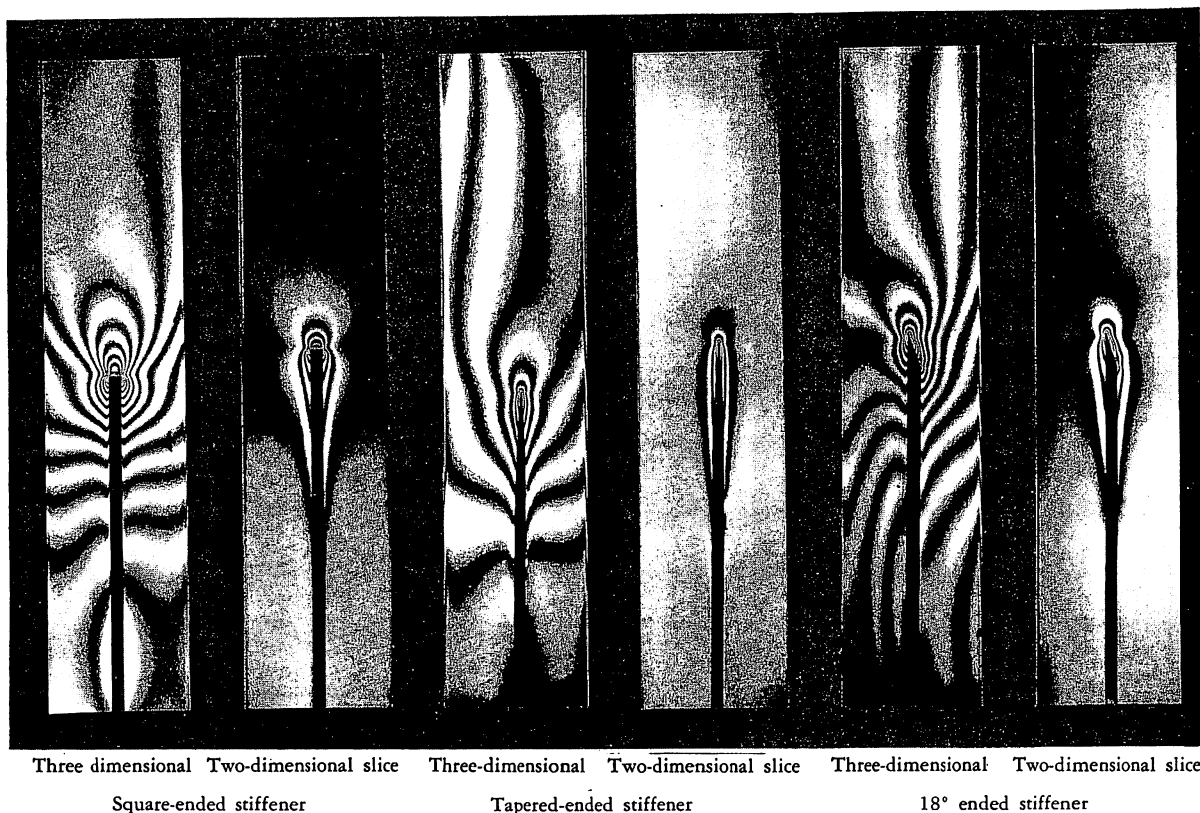


Figure 3. Photoelastic examples of the three-dimensional models and their associated two-dimensional slices.

diameters according to the stiffener end-shape. Finally, the normal stress in the matrix along the longitudinal axis of the stiffener was determined by the shear difference method. The stress concentration for this method reached its maximum value at the tip of the stiffener.

The data from the experiment are presented in the accompanying graphs (Figures 4-9). Each graph has a scaled drawing of the stiffener. The stresses along the critical direction are given in terms of concentrations ( $k$ ): the observed value at the point divided by the applied normal stress. All distances are normalized in terms of stiffener diameters ( $d_s$ ). For each configuration of stiffener there are two graphs. One shows the stresses in the longitudinal direction; the shear stress at the stiffener-matrix interface and the normal stress in the matrix along the stiffener axis.

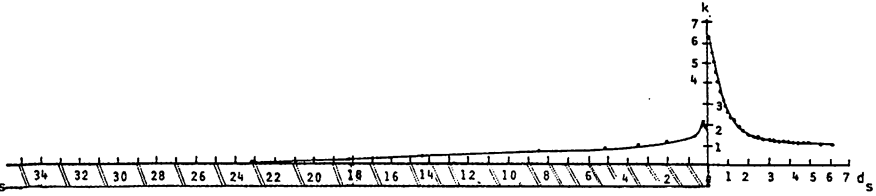


Figure 4. Square ended stiffener, longitudinal distribution of normal stress concentrations in the matrix under the tip of the stiffener and shear stress concentrations along the stiffener-matrix interface.

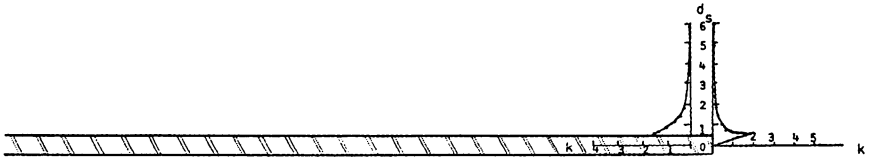


Figure 5. Square ended stiffener, radial distribution of shear stress concentrations across the region of the maximum gradient and the region of the widest range of influence.

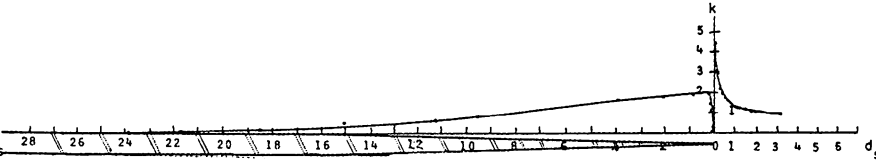


Figure 6. Tapered ended stiffener, longitudinal distribution of normal stress concentrations in the matrix under the tip of the stiffener and shear stress concentrations along the stiffener-matrix interface.

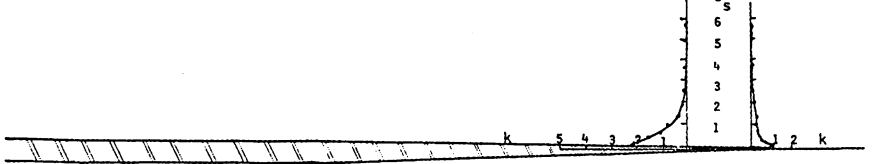


Figure 7. Tapered ended stiffener, radial distribution of shear stress concentrations across the region of the maximum gradient and the region of the widest range of influence.

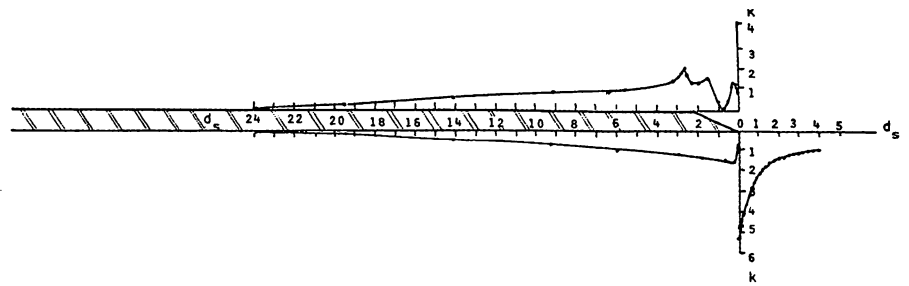


Figure 8. 18° ended stiffener, longitudinal distribution of normal stress concentrations in the matrix under the tip of the stiffener and shear stress concentrations along each side of the stiffener-matrix interface.

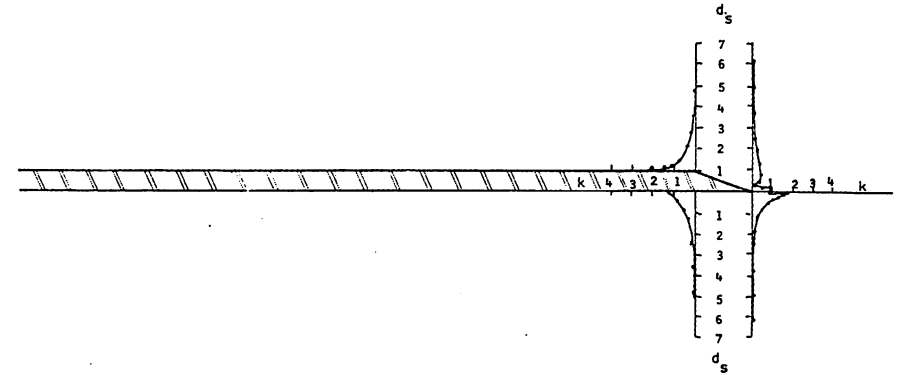


Figure 9. 18° ended stiffener, radial distribution of shear stress concentrations across the region of the maximum gradient and the region of the widest range of influence.

The other graph shows the radial shear stress concentrations along the direction of the maximum gradient and across the widest range of influence. The abscissas of the graphs locate the lines along which the stresses were determined and are shown in their relative positions with respect to the tip of the stiffener. Due to the lack of symmetry in the 18° ended stiffener, the stresses on both sides of the stiffener are shown in the graphs.

**Results and Discussion**

The first result of this experiment is that stress concentration appears to be highest in the case of the square ended stiffener and least in the tapered end. This is in general agreement with findings of other investigators. From a numerical standpoint there is one configuration where a comparison between investigators can be made: the case of the square ended stiffener under a tensile load. Tyson's work indicates that the maximum shear stress concentration along the stiffener was about 3.8:1, MacLaughlin obtained a value of 3:1, Schuster 2.5:1 and this investigator 2.2:1. Dow's theory predicts a maximum of 1.7:1 for this investigator's configuration. It should be noted that these are maximum values and they do not occur at the same location in each experiment. A better comparison of the results of each investigator can be made by examining the shear stress distributions along the stiffener (Figure 10).

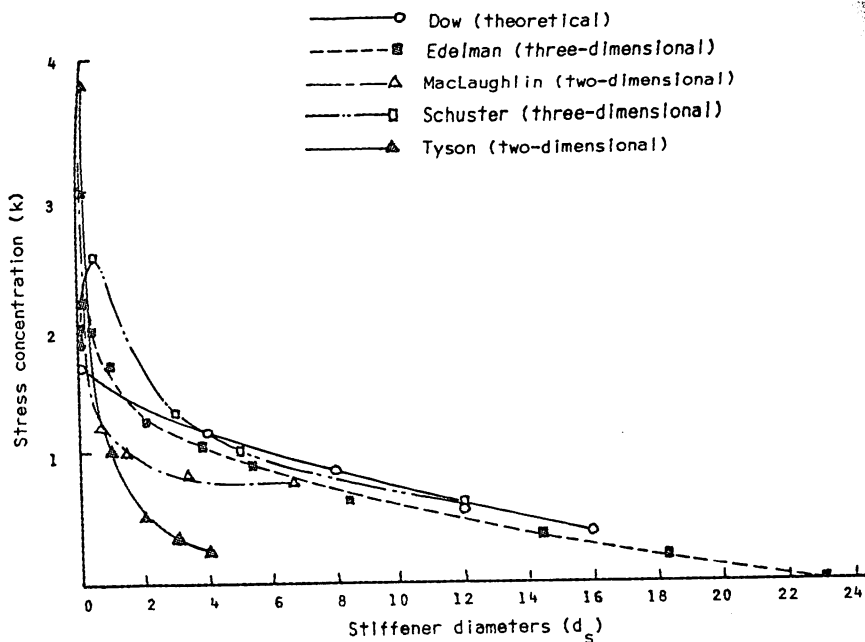


Figure 10. Shear stress along the matrix-stiffener interface as determined by five different investigators. Square ended stiffener under tensile loading.

When observed in this manner, it is readily seen that each of the photoelasticians obtained a higher maximum stress concentration than that predicted by Dow. This may well be due to the simplified end conditions used in Dow's theory. Also, in the photoelastic work, the two-dimensional models showed higher stress concentrations than the three-dimensional models. Even more important than the comparison of maximum values of stress concentrations is the shape of the distribution. The stress concentration in the two-dimensional models decreases very rapidly with increasing distance from the tip of the stiffener, while in the three-dimensional models the stress concentrations rise slightly and then decrease at a slower rate. When considering these results it should be remembered that each investigator changed more than one treatment used by the other investigators. Tyson and MacLaughlin used two-dimensional models. Schuster and this investigator used three-dimensional models. The ratios of elastic moduli ranged from 3000:1 in MacLaughlin's experiment, 150:1 in Schuster's, 20:1 in Tyson's and down to 5:1 in this experiment. In view of these and other differences it is surprising that the results show such close agreement.

Second, the ineffective or transfer length is relatively short with the stiffener carrying the full load within 25 diameters from the endpoint. This is in agreement with the theoretical developments of Dow. For the values of elastic moduli and areas selected for models used in this investigation, Dow predicted a minimum ineffective length of 20 diameters.

Third, in the matrix the range of influence of the stiffener drops off quite rapidly and falls to zero in the order of five or six diameters. This furnishes some information for use in determining the volume fraction of stiffeners necessary to provide adequate stiffening in the prototype material.

### Conclusions

In the models studied, the behavior of the stresses in the region surrounding the tip of the stiffener depends upon the geometry of the end shape. The maximum normal stress concentrations near the tip of the stiffener ranged from 4.5:1 in the case of the tapered end to 6.5:1 in the case of the square end. The maximum shear stress concentration at the stiffener-matrix interface was between 2.0:1 and 2.2:1 for all stiffener configurations. The ineffective or transfer length of all configurations occurred within 25 diameters of the stiffener endpoint.

### Literature Cited

- Dana, E. S. 1941. *Dana's Manual of Mineralogy*. 15th Edition. John Wiley. New York.  
 Designing strength into materials. December 17, 1966. *Business Week*, pages 91-98.  
 Dow, N. F. 1963. Study of stresses near a discontinuity in a filament-reinforced composite metal. General Electric Company, Valley Forge, Pennsylvania (R63SD61).  
 Edelman, W. E. To be published in *Experimental Mechanics*. A procedure for producing photoelastic models with rigid inclusions.  
 Krock, R., and R. Kelsey. February 1965. Whiskers—their promise and problems. *Industrial Research* 7:46-57.  
 MacLaughlin, T. F. 1966. Effect of fiber geometry on stress in fiber-reinforced composite materials. *Experimental Mechanics* 6:481-492.  
 Schuster, D. M., and E. Scala. 1964. The mechanical interaction of sapphire whiskers with a birefringent matrix. *Transactions of the AIME* 230:1635-1640.  
 Tyson, W. R., and G. J. Davies. 1965. A photoelastic study of the shear stresses associated with the transfer of stress during fibre reinforcement. *British Journal of Applied Physics* 16:199-205.

*Accepted for publication November 21, 1968.*